Toxicology 297 (2012) 1–9

Contents lists available at SciVerse ScienceDirect

Toxicology

journal homepage: www.elsevier.com/locate/toxicol

Assessing the relevance of *in vitro* studies in nanotoxicology by examining correlations between *in vitro* and *in vivo* data

Xianglu Han[a,*], Nancy Corson[a], Pamela Wade-Mercer[a], Robert Gelein[a], Jingkun Jiang[c], Manoranjan Sahu[d], Pratim Biswas[d], Jacob N. Finkelstein[b,a], Alison Elder[a], Günter Oberdörster[a]

[a] Department of Environmental Medicine, University of Rochester, Rochester, NY, USA
[b] Departments of Pediatrics and Radiation Oncology, University of Rochester, Rochester, NY, USA
[c] State Key Joint Laboratory of Environment Simulation and Pollution Control, School of Environment, Tsinghua University, Beijing, China
[d] Department of Energy, Environmental and Chemical Engineering, Washington University in St. Louis, St. Louis, MO, USA

ARTICLE INFO

Article history:
Received 6 January 2012
Received in revised form 23 February 2012
Accepted 23 March 2012
Available online 2 April 2012

Keywords:
Nanoparticle
TiO_2
LDH
Protein carbonylation
Dose–response analysis
Sigmoidal
Steepest slope

ABSTRACT

There is an urgent need for *in vitro* screening assays to evaluate nanoparticle (NP) toxicity. However, the relevance of *in vitro* assays is still disputable. We administered doses of TiO_2 NPs of different sizes to alveolar epithelial cells *in vitro* and the same NPs by intratracheal instillation in rats *in vivo* to examine the correlation between *in vitro* and *in vivo* responses. The correlations were based on toxicity rankings of NPs after adopting NP surface area as dose metric, and response per unit surface area as response metric. Sizes of the anatase TiO_2 NPs ranged from 3 to 100 nm. A cell-free assay for measuring reactive oxygen species (ROS) was used, and lactate dehydrogenase (LDH) release, and protein oxidation induction were the *in vitro* cellular assays using a rat lung Type I epithelial cell line (R3/1) following 24 h incubation. The *in vivo* endpoint was number of PMNs in bronchoalveolar lavage fluid (BALF) after exposure of rats to the NPs *via* intratracheal instillation. Slope analyses of the dose response curves shows that the *in vivo* and *in vitro* responses were well correlated. We conclude that using the approach of steepest slope analysis offers a superior method to correlate *in vitro* with *in vivo* results of NP toxicity and for ranking their toxic potency.

1. Introduction

The exciting field of nanotechnology has seen a rapid expansion in recent years. However, there is a growing concern about potential risks posed by the technology due to exposure of humans and the environment (Stern and McNeil, 2008).

Current toxicological research on nanotechnology mainly focuses on the adverse effects of one of the building blocks of the technology – nanoparticles (NPs). There are several challenges that seem to be special to nanotoxicology when evaluating the adverse effects of NPs. One challenge is whether to use mass as a dose metric for assessing NP toxicity. Since the activity of NPs is determined to a large extent by NP surface properties, there has been efforts to determine if a dose metric based on surface area is preferable rather than one based on mass (Brown et al., 2001; Oberdörster et al., 2005a,b, 2007; Teeguarden et al., 2007; Monteiller et al., 2007; Wittmaack, 2007; Stoeger et al., 2007).

Another challenge is to validate *in vitro* assays that have been well established for assessing toxicity of chemicals. There is an urgent need for quick and reliable *in vitro* screening assays to replace or reduce the slow, costly and ethically controversial animal testing that might be required due to the rapid development and commercialization of nano-enabled products. However, some traditional *in vitro* assays have been found to generate misleading results because some of the nanomaterials could interfere with the assays (Wörle-Knirsch et al., 2006; Casey et al., 2007; Belyanskaya et al., 2007; Han et al., 2011). In addition, NPs, because of their large specific surface area, could adsorb essential nutrients in cell culture medium, making it difficult to interpret some cytotoxicity results (Guo et al., 2008).

When evaluating NP toxicity using *in vitro* assays, *in vivo* relevance is an essential criterion for accepting their utility. The *in vivo* relevance can be questioned because of the differences between *in vitro* and *in vivo* conditions. These differences warrant developing novel methods to define equivalent doses between *in vitro* and *in vivo* exposures in order to improve correlations between the two testing systems.

One difference is the high concentrations/dose used in most traditional *in vitro* studies. An extremely high dose rate (dose administered per unit of time) is another issue of *in vitro* studies

* Corresponding author at: Department of Environmental Medicine, University of Rochester, 575 Elmwood Ave., MRBx Building, Box 850, Rochester, NY 14642, USA. Tel.: +1 989 638 8168; fax: +1 989 638 9933.
E-mail address: XHan2100@gmail.com (X. Han).

0300-483X/$ – see front matter © 2012 Elsevier Ireland Ltd. All rights reserved.
http://dx.doi.org/10.1016/j.tox.2012.03.006

because the full dose is delivered as a bolus in traditional *in vitro* assays. The dose rate in such studies is much higher than in *in vivo* inhalation studies in which animals are exposed to a low concentration of chemical or particle *via* inhalation for an extended period of time (hours, days, weeks, or longer). Another important difference is the wide use of dispersants *in vitro* but not necessarily *in vivo* (*e.g.*, inhalation of pristine NPs generated from dry powders) (Park et al., 2009). NPs dispersed in cell culture medium would adsorb some components in the medium while NPs inhaled into the lung would adsorb components of pulmonary surfactant. However, the use of high doses and high dose rates *in vitro* by itself does not invalidate *in vitro* assays. The *in vitro* data could still be useful as long as the data are confirmed to correlate well with *in vivo* results. In particular, *in vivo* dosing of the respiratory tract by intratracheal instillation or oro-pharyngeal aspiration are also bolus-type delivery methods and results should correlate better with *in vitro* dosing.

There have been some studies that addressed the issue of the *in vivo* relevance of some *in vitro* assays for evaluating the toxicity of NPs (Sayes et al., 2007) or ambient particulate matter (Seagrave et al., 2005). Both found poor correlations. However, these findings do not necessarily indicate intrinsic flaws of the *in vitro* assays for predicting *in vivo* toxicity. Instead, there can be multiple reasons for the differences between *in vitro* and *in vivo* results (Seagrave et al., 2005). Our group (Rushton et al., 2010) has proposed an alternative approach of slope analysis and found a good *in vitro–in vivo* correlation when applied to the data in the paper of Sayes et al. (2007).

The objective of this work is to test the hypothesis that results of *in vitro* assays correlate with acute *in vivo* effects when an appropriate response metric is used. Therefore, in this work, we continue to address the relevance of *in vitro* assays by comparing results of *in vitro* and *in vivo* studies for NPs of different sizes based on a slope analysis of dose–response curves. In addition to the graphical method used in our previous work to determine the maximum response per unit of the dose (steepest slope) (Rushton et al., 2010), we introduce a new method to derive the steepest slope – a mathematical method. We report in this work that using this approach showed a good correlation of acute toxicity between *in vitro* and *in vivo* results. Future work needs to also consider extension to long-term effects.

2. Methods

2.1. Materials

NPs used for the main study of this work includes different TiO_2 NPs (for correlation study), and for assay validation only a silver NP, and a copper NP. A series of anatase TiO_2 NPs of different sizes (3, 7, 10, 16, 30, 50, 53, and 104 nm) were used for the correlation study. These NPs were synthesized from titanium tetra-isopropoxide (TTIP, 97%, Aldrich) either in a diffusion or premixed flame aerosol reactor (Jiang et al., 2007). These two methods for preparing NPs are commonly used, although it was unknown if both methods could generate particles with different toxicological activities. Thus, NPs generated by both methods were considered as different NPs even if they had the same average size. The other NPs (P-25, TIO_2, Ag-40, and Cu-40) were only used for validating the protein carbonylation/oxidation assay (see Supplemental Information).

2.2. Physicochemical characterization of NPs

The hydrodynamic sizes of the anatase TiO_2 NPs in different media were measured using dynamic light scattering (DLS) technology (intensity distribution of suspended NPs) with a Malvern ZetaSizer (ZetaSizer Nano ZS). Number or volume distribution of the particles would generally incur larger errors because they are not direct measurements; instead, they are derived from the directly measured intensity distribution. The NPs were sonicated using a cuphorn sonicator for 15 s twice (Sonics VCX 750 with maximum output 750 W and a frequency of 20 kHz, Newtown, CT) at 29% maximum output. Suspension and cell culture media included saline (pH 5.9), phosphate buffered saline (PBS) with a pH of 7.4 (1.14 g of Na_2HPO_4, 0.72 g of NaH_2PO_4, and 8.18 g of NaCl in deionized water, pH adjusted to 7.4 using 10 N NaOH), RPMI 1640 cell culture medium with no phenol red (Invitrogen GIBCO® 11835), and RPMI medium containing 1% fetal bovine serum (FBS, Hyclone, SH30070.03). For each size of anatase TiO_2 NP, the same concentration was used (2 μg/ml). Measurements were repeated at least 6 times to ensure a stable reading; if not, measurements would be repeated further until there is no obvious time trend of the measured sizes as judged by examining the last 6 measurements. In addition, primary particle sizes and agglomeration state were also measured using transmission electron microscope. BET isotherms (Autosorb-1, Quantachrome) were used to determine the specific surface area of the NPs (Brunauer et al., 1938).

2.3. Rationale of choosing in vitro and in vivo endpoints

There is increasing evidence that the induction of oxidative stress through generation of reactive oxygen species (ROS) plays a critical role in the mechanism of toxicity induced by NPs (Brown et al., 2001; Xiao et al., 2003; Hussain et al., 2005; Nel et al., 2006; Long et al., 2006; Sayes et al., 2006; Federici et al., 2007; Limbach et al., 2007). Based on this, most of the endpoints we selected for the *in vitro* and *in vivo* analyses were related to oxidative stress or inflammation. The oxidative stress related endpoints in three testing systems were ROS generation in a cell-free system, protein carbonylation in cultured cells, and the number of polymorphonuclear neutrophils (PMNs) in lung lavage fluid. In addition, we also included measurement of released lactate dehydrogenase (LDH) from cultured cells. Though LDH release is caused by cellular membrane damage which may or may not be related to oxidative stress, the LDH assay is a very commonly used assay and warrants evaluation for rapid screening of NP toxicity. TiO_2 particles could interfere with the LDH assay by adsorbing LDH molecules (Han et al., 2011), however, there is only minor interference at low and intermediate concentration so the assay will still be useful as long as its *in vivo* relevance *can be shown*.

The endpoints chosen for this study are general and broad-based because the purpose is to choose relatively simple screening assays that are widely applicable so that the toxicity of a large number and variety of different NPs can be evaluated.

2.4. Cell-free ROS assay

The intrinsic capability of the NPs in generating reactive oxygen species (ROS) was evaluated using a cell-free ROS assay (Jiang et al., 2008). The assay was performed in the dark to avoid any interference from photocatalytic activities of the NPs. The dye 2′,7′-dichlorofluorescein diacetate (DCFH-DA) (CalBiochem, 287810) is deacetylated and oxidized into a fluorescent product in the presence of NP-generated free radicals. The fluorescence was detected using a spectrofluorometer (absorbance/emission maxima, 485 nm/535 nm).

Three to six groups (including controls) were used for these NPs with concentration ranges from 0 to 100 μg/ml and a dose spacing factor of 2 or 3. When expressed as NP surface area, the highest concentration of 100 μg/ml is equivalent to 30 cm^2/ml for the largest TiO_2 NP and 426 cm^2/ml for the smallest NP. Since ROS level in the cell-free assay increased linearly with increasing NP concentration (see Section 3), the slope of this increase for each NP was obtained using linear regression. In addition to mass concentration (μg/ml), surface area concentration (cm^2/ml) was also used to express the slopes. After calculating the mass based slope for each NP, the surface area based slope was calculated by dividing the mass based slope by the specific surface area (SSA) of the NP.

2.5. Cell culture

A rat lung epithelial Type I like cell line, R3/1 (Koslowski et al., 2004), was used for the cellular *in vitro* studies. Cells were maintained in RPMI 1640 cell culture medium (without phenol red) containing 10% fetal bovine serum (FBS) and passaged every three or four days. For *in vitro* assays, cells with a density of 10^5 per ml were seeded in plates, grown to subconfluency (70–80% confluency), and exposed to NPs in RPMI 1640 with 1% FBS for different time durations. Though plates with wells of different sizes (6-, 12-, or 24-well plate) were used, when seeding cells into a plate, the same cell density was used and a constant depth of cell culture medium was maintained. NPs were probe sonicated in RPMI 1640 with 1% FBS on ice for 10 s twice.

2.6. LDH assay

The LDH assay was performed according to the Sigma LDH assay kit. The assay works by measuring the catalytic activity of LDH in the reaction: $NADH + Pyruvate \leftrightarrow NAD^+ + Lactate$, where NADH stands for reduced β-nicotinamide adenine dinucleotide. The decreasing rate of NADH – measured as decreasing absorbance at 340 nm over 2 min – is used as an indicator of LDH activity.

Eight groups (including controls) were used for this study with concentrations ranging from 0 to 200 μg/ml for larger particles (50 nm), 0–100 μg/ml for medium sized particles (10 nm and 30 nm), and 0–50 μg/ml for smaller particles (3 and 7 nm). The spacing factor was 2 or 2.5.

2.7. Protein carbonylation study

In this study, enzyme-linked immunosorbent assay (ELISA) was used for detecting protein carbonyls following their reaction with dinitrophenylhydrazine (DNPH) (Buss et al., 1997).

The materials and their sources were as follows: protease inhibitors (Sigma, P2714), ascorbic acid (Sigma, 255564), ferrous ammonium sulfate (Sigma, 215406), bovine serum albumin (BSA, Sigma, A9056), $NaBH_4$ (Sigma, 213462), 2,4-dinitrophenylhydrazine (Sigma, D199303), 3,3,5,5-tetramethylbenzidine (TMB) tablet (Sigma, T-3405), hydrogen peroxide (H_2O_2, 30%) (Sigma, H-1009), guanidine hydrochloride (Sigma, G3272), anti-DNP antibody (Sigma, D-9656), anti-rabbit antibody HRP-linked IgG (Cell Signaling Technology, 7074), flat ELISA plate (high binding, Greiner bio-one, 756071), filter (Pall Life Sciences, 0.2 μm Super Membrane), EDTA disodium salt (J. T. Baker, 8993-1), phosphoric acid (85%) (EM Science, PX0995-13), 2 N HCl diluted from concentrated HCl (Seastar), NaOH (J. T. Baker, 3722-04), Na_2HPO_4 (S0876), NaH_2PO_4 (S0751), and citric acid (Sigma 251275). Phosphate buffered saline (PBS) contains 10 mM phosphate buffer (8 mM of Na_2HPO_4 and 2 mM of NaH_2PO_4) in 140 mM NaCl with a pH of 7.4. DNPH solution contains 10 mM DNPH in 6 M guanidine hydrochloride and about 0.29 M potassium phosphate buffer with a pH of 2.5.

The bicinchoninic acid (BCA) assay was used to measure protein concentration for the samples as described in the next section. Based on the measured values, protein concentrations were adjusted to 1 mg/ml for reaction with 10 mM DNPH in a volume ratio of 1:3. Subsequent ELISA steps follow the paper by Buss et al. (1997), except that some antibodies and a few reagents were suggested in another paper (Alamdari et al., 2005).

Eight groups (including controls) were used for this study with dose range from 0 to 200 μg/ml for larger particles (50 nm), 0–100 μg/ml for medium sized particles (10 and 30 nm), and 0–50 μg/ml for smaller particles (3 and 7 nm). Dose spacing factor was 2 or 2.5.

2.8. The bicinchoninic acid (BCA) assay

The BCA assay was used to measure protein concentration for the carbonylation samples and total protein levels of lung lavage fluid samples. It was based on a kit from Thermo Scientific (Thermo Scientific Pierce BCA Protein Assay, PI-23235).

2.9. Animal studies

Male Fischer 344 rats were purchased from Harlan Laboratories and housed in the University Medical Center animal facilities. All procedures were approved by the University Committee on Animal Resources (UCAR) of the University of Rochester.

Rats had body weights ranging about 250–300 g and were divided into four groups (three dose groups and a control group) with a group size of three or four rats (see Fig. 9 for doses). NPs were dispersed in a sterile physiological saline (Hospira, NDC 0409-4888-10), probe sonicated for 10 s, and immediately given to animals *via* intratracheal instillation.

The rats were sacrificed 24 h after intratracheal instillation to evaluate pulmonary inflammation. Euthanasia was induced with an i.p. injection of 0.3–0.5 ml of sodium pentobarbital (64.8 mg/ml, Hospira, NDC 67384-501-52).

The lungs were lavaged 5 times with 5 ml sterile saline (sodium chloride injection, UPS 0.9% sterile from Abbott Labs, North Chicago, IL 60064) each time. The 1st and 2nd lavage fluid was put into a 15 ml polypropylene centrifuge tube. The 3rd–5th lavage fluid was placed in a 50 ml polypropylene tube. The supernatant from lavages 3–5 was discarded while that from lavages 1 to 2 was saved (aliquots of 100 μl, −20 °C) for measuring protein level and same day analysis of LDH and β-glucuronidase (400 μl, 4 °C). The pellets from both tubes were resuspended in 0.9% NaCl and combined in a final volume of 10 ml. The suspension was used for differential cell counts (PMNs and other cells) and viability measurements.

The β-glucuronidase activity in BALF was determined by measuring its activity in the reaction 4-nitrophenyl-glucuronide ↔ p-nitrophenol + monosaccharide (Stahl and Fishman, 1984). LDH was measured according the method described in Section 2.6. Protein levels were measured using the BCA method described in Section 2.8.

2.10. Dose- and response-metrics

The issue of response metric is related to the shape of a dose–response curve. At the point with the steepest slope (Fig. 1a), a slight increase in dose leads to a remarkable increase in response. In this work, "steepest" slope and "maximum" slope are used interchangeably. The word "maximum" is often used in mathematics while "steepest" seems to be more instinctive when using the graphical method as described below.

To determine the steepest slope, two methods were used: a graphical method and a mathematical method. In the graphical method, the response data are plotted against the dose, the slope for each pair of adjacent dose groups is calculated by dividing the response difference by the dose difference, and the largest slope is selected. The response difference is the difference between the two average responses of the two adjacent dose groups. To get a confidence interval for the steepest slope, all the individual data points in the two dose groups are used for a linear regression analysis.

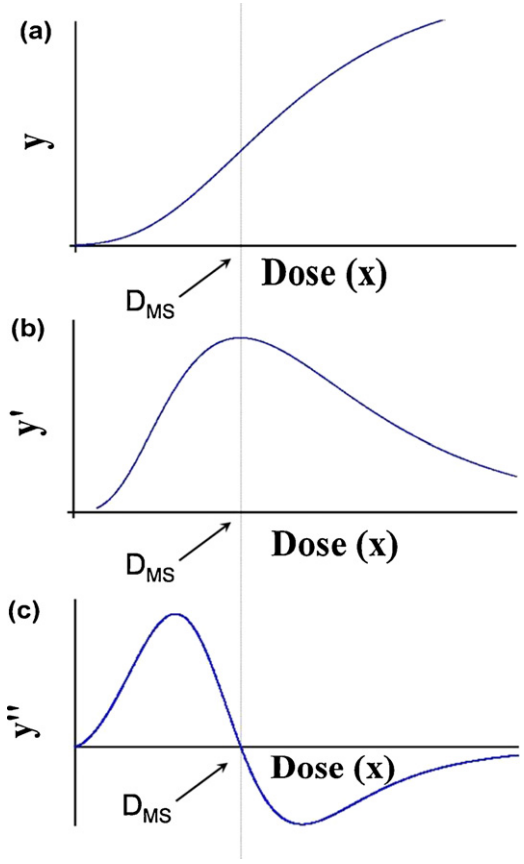

Fig. 1. Calculation of the steepest slope using the mathematical method. (a) Fit a dose–response curve and get $y = f(x)$. (b) Take the first derivative $y' = f'(x)$ and solve the equation. (c). Obtain the second derivative $y'' = f''(x)$, solve the equation, let it be zero, and get x, which is actually D_{MS}, the dose where the maximum slope is attained. Put D_{MS} back into y' and obtain the steepest slope.

In the mathematical method (Fig. 1), the first step is to fit a sigmoidal curve for dose–response data wherever it is appropriate, from which an equation is obtained:

$$y = b + \frac{t - b}{1 + 10^{h(\log\ ED_{50} - \log x)}} \tag{1}$$

where y is response; b is bottom, *i.e.*, the background level of response; t is Top, meaning the maximum response that can be asymptotically obtained as dose increases indefinitely; h is the hill slope, the steepness factor of the curve when taking logarithm on dose x; and ED_{50} is the dose to attain half of the maximum response after adjusting for background response.

Subsequently, the first derivative of Eq. (1) with respect to dose x is calculated to get an equation corresponding to the so-called "slope curve":

$$y' = h(t - b)\frac{ED_{50}^{h} x^{h-1}}{\left(x^{h} + ED_{50}^{h}\right)^{2}} \tag{2}$$

To get the maximum value of the "slope curve", derivative is taken from Eq. (2) (*i.e.*, to get the second derivative of Eq. (1), y''; y'' is still a function of the dose x, the complex formula for y'' is not shown since it is not used for routine calculation). By solving $y'' = 0$, the dose where the steepest slope gets across (D_{MS}, dose for maximum slope) is obtained (Eq. (3)). D_{MS} exists only when the Hill slope in Eq. (1) is larger than one (*i.e.*, $h > 1$), which is evidenced by its relationship with ED_{50}:

$$D_{MS} = \left(\frac{h - 1}{h + 1}\right)^{1/h} ED_{50} \tag{3}$$

Finally, the maximum slope (MS) is obtained by putting D_{MS} as a value of x into Eq. (2). The value of y' obtained is MS (Eq. (4)).

$$MS = \frac{(t - b)(h - 1)^{1-1/h}(h + 1)^{1+1/h}}{4hED_{50}} \tag{4}$$

Note that though multiple equations were given to show the process, only Eq. (4) is needed for using the mathematical method. MS will be obtained as long as t, b, h, and ED_{50} are obtained *via* curve fitting of a sigmoidal curve.

With the steepest slopes obtained, a toxicity comparison can now be conducted by comparing these slopes, with a higher value meaning higher toxicity. Note that

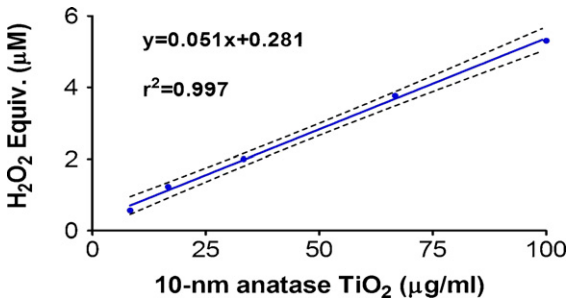

Fig. 2. Dose–response curve of ROS data for a 10 nm anatase TiO_2 NP in a cell-free system showing the calculation of slope *via* linear regression. The slope obtained was 0.051 μM H_2O_2 equivalent per μg/ml. The ROS were measured in a cell-free system (sodium phosphate buffer) using the dye 2′,7′-dichlorofluorescein diacetate (DCFH-DA). The fluorescence was measured using a spectrofluorometer with excitation/emission wavelengths of 485 nm/535 nm. The assay was performed in the dark to avoid any interference from photocatalytic activities of the NPs.

no matter which criterion is used for ranking toxicity (benchmark dose, ED_{50}, or slope), there are always exceptions. There is no guarantee that ranking based on one criterion is completely consistent with that of another.

2.11. Correlation between in vitro and in vivo data

The correlation coefficient between two endpoints can be calculated using the slope data when data of the two endpoints are available for a sufficient number of NPs. Since no evidence of normal distribution is present, the slope data was analyzed using a non-parametric method (Spearman correlation).

2.12. Statistical analysis

Dose–response modeling and correlation analyses were performed using the software GraphPad Prism 5 (GraphPad Software, La Jolla, CA, USA) while other calculations were completed in Microsoft Excel spreadsheet. When using the mathematical method for obtaining the steepest slopes for protein carbonylation data, raw data were first normalized by dividing each data point by the average of the control group so that a fixed "bottom" value of 1 for fitting. This was not done for LDH data because LDH data have a meaningful unit while protein carbonylation readings do not. A statistical test was considered significant when p 0.05. Confidence intervals (CIs) were calculated for the steepest slopes in different ways for the graphical and mathematical methods. For ROS data, the slopes were obtained with CIs *via* linear regression. In the graphical method for the *in vivo* data, CIs were also obtained *via* linear regression for the data of the two dose groups that the steepest slope was based on. In the mathematical method for the LDH and protein oxidation data, each of the CIs for the slopes was obtained by manually resampling the dose–response data using Jackknife technique (randomly deleting one data point each time to get a sample for slope calculation).

3. Results

3.1. NP characterization

Hydrodynamic sizes were found to be much larger than the particle sizes in dry state (Table 1). The size measurements in PBS and in RPMI 1640 cell culture medium were similar with the latter slightly larger. As expected, the measured sizes of the NPs were remarkably smaller in RPMI medium with presence of 1% FBS than without due to coating of NPs (about 70% reduction in size).

3.2. Cell-free ROS data

All anatase TiO_2 NPs showed a dose-dependent linear increase in generating ROS, a typical example is shown for a 10 nm TiO_2 NP prepared using the diffusion flame method (Fig. 2). Therefore, the slopes were obtained *via* linear regression. The slopes increased with increasing NP sizes based on NP surface area as a dose metric while there was no clear trend when the slopes are based on mass (Fig. 3).

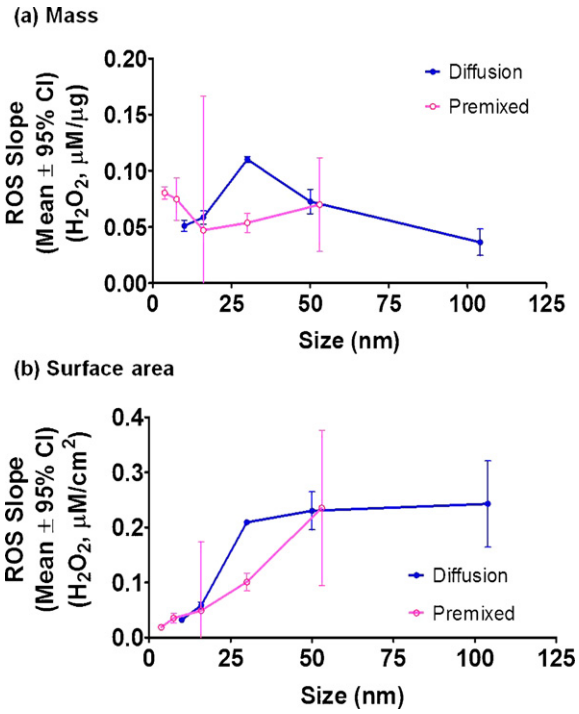

Fig. 3. Slopes of cell-free ROS data *versus* particle size (nm) for the TiO_2 NPs. Each of these slopes was obtained from a dose–response dataset *via* linear regression with an example shown in Fig. 2. The slopes have a unit of μM H_2O_2 equivalent per μg/ml based on mass or μM H_2O_2 equivalent per cm^2/ml based on surface area. While there is no clear trend for slope expressed in mass (a), surface area based slope increases with increasing size (b). These NPs were either prepared by a diffusion flame or a premixed flame method.

3.3. LDH data

The 24 h LDH dose–response data for all the anatase TiO_2 NP showed sigmoidal curves with a 30 nm anatase NP as an example (Fig. 4). The mathematical method was used for calculating the steepest slopes and the slopes were plotted against NP size (Fig. 5). As can be seen, the slope increased as a function of NP size when based on surface area but not on mass.

3.4. Protein carbonylation data

An example for the carbonylation data was presented using a 30 nm anatase NP (Fig. 6). The steepest slopes were obtained by the mathematical method and plotted against NP size either based on

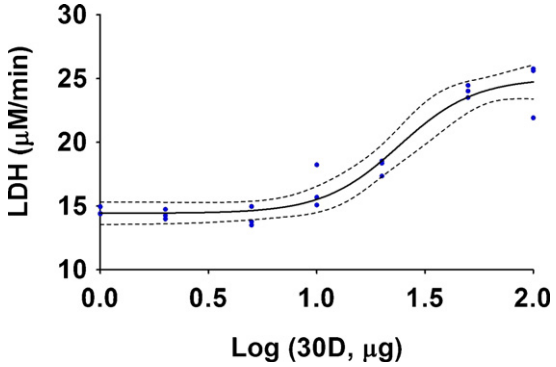

Fig. 4. LDH dose–response data (mass dose) for an antase TiO_2 NP (30 nm, diffusion flame) fitted using a sigmoidal equation in GraphPad Prism. The 24 h LDH data (cultured R3/1 cells) were plotted against the logarithm of dose (μg/ml). The steepest slope was obtained using the mathematical method described in Fig. 1.

Table 1
Physicochemical characterization of the anatase TiO_2 NPs. Primary particle sizes and size distributions of the NPs were measured using transmission electron microscopy (TEM). Hydrodynamic sizes and size fluctuations over time were measured using dynamic light scattering (DLS) technology. The data are based on size distribution by Intensity (of the scattered light measured). Specific surface area (SSA) was measured using the Brunauer–Emmet–Teller (BET) method. Particle sizes were also calculated based on SSA. These anatase NPs were prepared with titanium tetra-isopropoxide (TTIP, 97%, Aldrich) using a diffusion flame or premixed flame method. In the diffusion method, the oxidizer (O_2) combines with the fuel (methane, CH_4) by diffusion. A premixed flame is a flame in which the oxidizer is mixed with the fuel before it reaches the flame front.

Preparation method (type of flame)	Calculated size (nm) based on SSA	TEM size (nm, mean ± SD)	Hydrodynamic size in medium (nm, mean ± SD)				SSA (m^2/g)
			Saline (pH 5.9)	PBS (pH 7.4)	RPMI 1640	RPMI with 1% FBS	
Diffusion	10	11 ± 3	778 ± 11	704 ± 15	1008 ± 17	186 ± 6	157.10
Diffusion	16	17 ± 5	906 ± 14	705 ± 16	643 ± 12	183 ± 6	100.00
Diffusion	30	29 ± 10	702 ± 10	541 ± 9	590 ± 14	191 ± 8	52.56
Diffusion	50	47 ± 13	631 ± 8	537 ± 14	592 ± 9	237 ± 7	31.52
Premixed	3	5 ± 1	879 ± 13	887 ± 21	903 ± 20	211 ± 6	426.1
Premixed	7	7 ± 3	869 ± 15	825 ± 11	822 ± 13	189 ± 10	209.6
Premixed	16	16 ± 6	844 ± 12	704 ± 17	813 ± 15	196 ± 7	95.8
Premixed	30	24 ± 9	841 ± 13	650 ± 10	783 ± 14	188 ± 7	53.10
Premixed	53	49 ± 21	763 ± 11	530 ± 9	586 ± 19	212 ± 9	29.68

mass or surface area (Fig. 7), showing again that the slope increased as a function of NP size when based on surface area but not mass.

3.5. *In vivo study*

Rats were exposed to the anatase TiO_2 NPs for 24 h at three different doses *via* intratracheal instillation and several endpoints were measured 24 h later. Compared to other endpoints (data in supplementary information, Figs. S-2–S-13), the number of PMNs in bronchoalveolar lavage fluid (BALF) was the most sensitive indicator of pulmonary inflammation and showed clear dose–response relationships (Fig. 8). The PMN dose–response curves had a general trend of decreasing steepness of slope with increasing NP size when based on mass as a dose metric, while the trend was generally reversed based on surface area. Using the graphical method, the slopes for all these NPs were obtained and plotted against NP size (Fig. 9). These slopes increase as a function of NP size based on surface area (maximum response per cm^2 surface area of NP) but decrease based on mass (maximum response per μg of NP).

3.6. *Correlations between in vitro and in vivo data based on the steepest slope*

For the anatase NPs, correlations between the *in vitro* data (cell-free ROS data, cellular LDH data, and cellular protein carbonylation data) and *in vivo* data (number of PMNs in rat BALF) were correlated based on slopes derived from the corresponding dose–response data. These slopes were either calculated on the basis of mass or surface area as dose metric.

Correlations between slopes of the ROS data (Fig. 3) and those of PMN data (Fig. 9) were plotted in Fig. 10, either based on mass or surface area. Similarly, correlations between slopes from LDH data (Fig. 5) and those from PMN data (Fig. 9) were plotted in Fig. 11. Fig. 12 shows the correlations between slopes from protein carbonylation data (Fig. 7) and slopes from PMN data (Fig. 9).

In all three cases, positive correlations with statistical significance were found between the *in vitro* and *in vivo* data when using surface area based dose- and response-metrics (Figs. 10–12). On the other hand, when examined on a mass basis, none of the correlations had statistical significance.

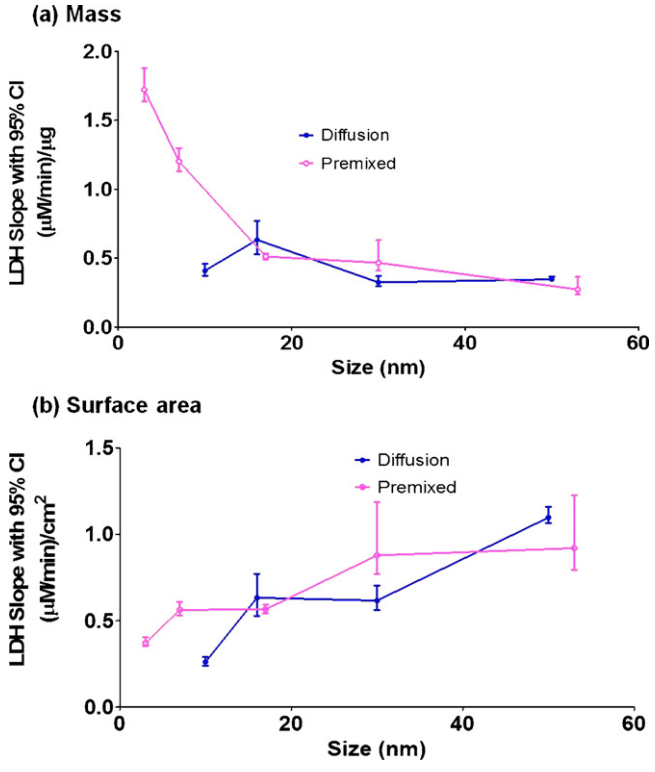

Fig. 5. Slopes of the *in vitro* LDH data from exposure study in R3/1 cells for the anatase TiO_2 NPs (mathematical method). While there is a decreasing trend with increasing NP size for slopes expressed in mass (unit: μM/min LDH activity per μg/ml mass concentration) (a), surface area (unit: μM/min LDH activity per cm^2/ml mass concentration) based slopes increase with increasing NP size (b). These NPs were prepared by a diffusion or a premixed flame method.

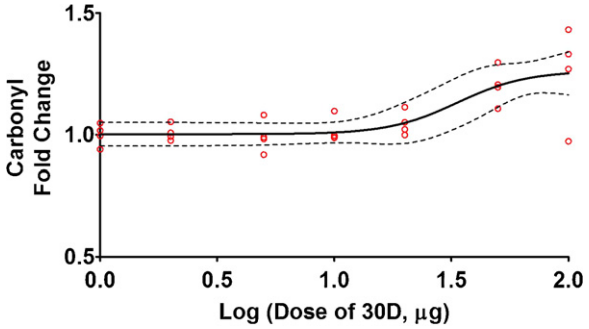

Fig. 6. Dose–response data (mass dose) of protein carbonylation following exposure of R3/1 cells. The protein carbonyl level increases in a dose-dependent manner after 24 h exposure. Carbonyl values were normalized with respect to the average value of the control group (average of control was set as 1). This example is about a 30 nm anatase TiO_2 NP (prepared by a diffusion flame method).

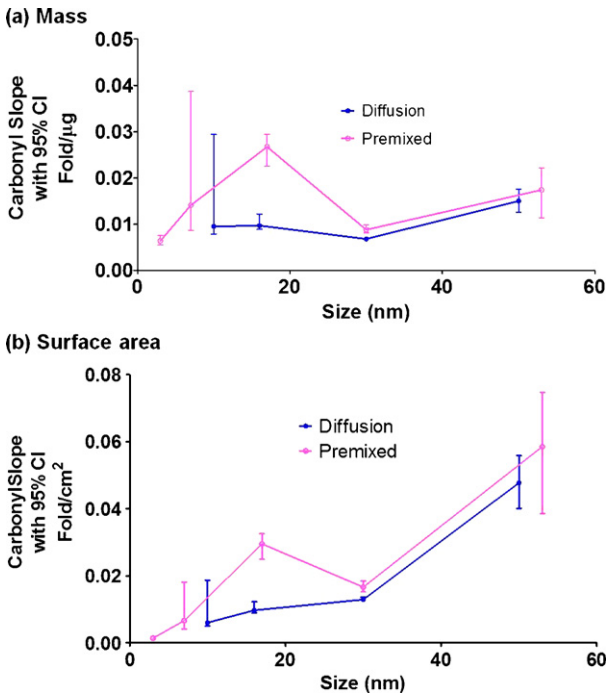

Fig. 7. Slopes of the *in vitro* protein carbonylation data from the anatase TiO_2 exposure study in R3/1 cells (mathematical method). Each of these slopes was obtained from a dose–response dataset with an example dataset shown in Fig. 6. While there is no clear trend for slope expressed in mass (unit: fold increase of carbonyl per μg/ml) (a), surface area based slopes (unit: fold increase of carbonyl per cm^2/ml) increase with increasing NP size (nm) (b). These NPs were prepared using diffusion (marked with "D") or premixed flame method (marked with "P").

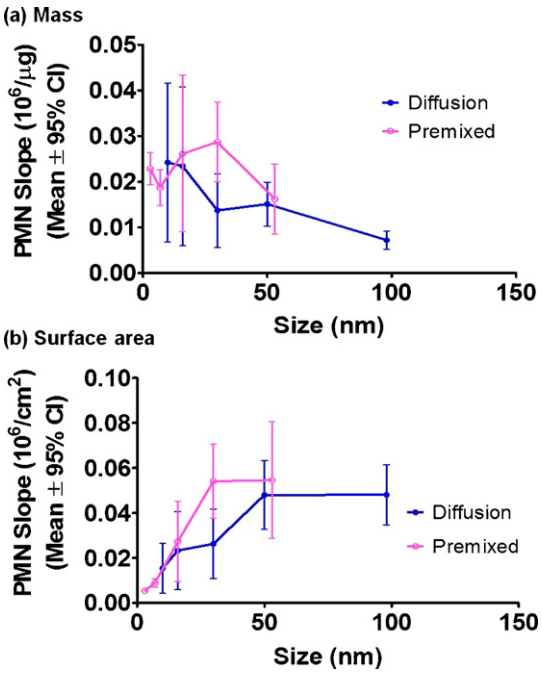

Fig. 9. Slopes of PMN data from the anatase TiO_2 exposure study in rats as a function of particle size (graphical method). Each of the slopes was obtained using a graphical method in which the largest slope from a dose–response curve was picked directly from the slopes of adjacent pairs of dose groups. While there is a decreasing trend for slope expressed in mass (10^6 PMNs per μg/rat) (a), surface area based slope (10^6 PMNs per cm^2/rat) increases with increasing size (b). These slopes will be used as *in vivo* data for correlating with *in vitro* slopes. These NPs were prepared using diffusion (marked with "D") or premixed flame method (marked with "P").

4. Discussion

The major focus of this work is to assess the usefulness of *in vitro* (cell-free and cellular) assays by examining the correlations between the *in vitro* and *in vivo* data while using either NP mass or NP surface area as a dose metric and the steepest slope of the dose–response curve (maximum response per unit dose) as a response metric. The analysis showed that only the dose metric "surface area" showed a significant correlation between *in vitro* and *in vivo* results.

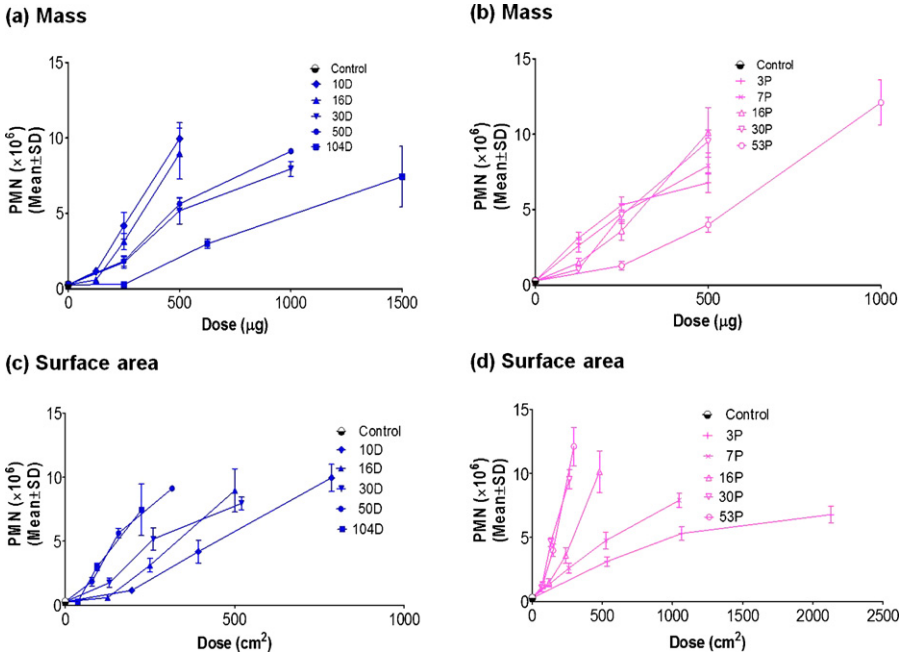

Fig. 8. PMN number in rat bronchoalveolar lavage fluid 24 h after intratracheal instillation of the anatase TiO_2 NPs (dose unit: μg or cm^2 per rat). There is a clear response for all NPs and many dose–response curves level off at high-dose end, suggesting that PMN number is a sensitive marker for acute lung inflammation and it can serve as the *in vivo* endpoint for correlating with *in vitro* data. The NPs were prepared using diffusion (marked with "D") or premixed flame method (marked with "P").

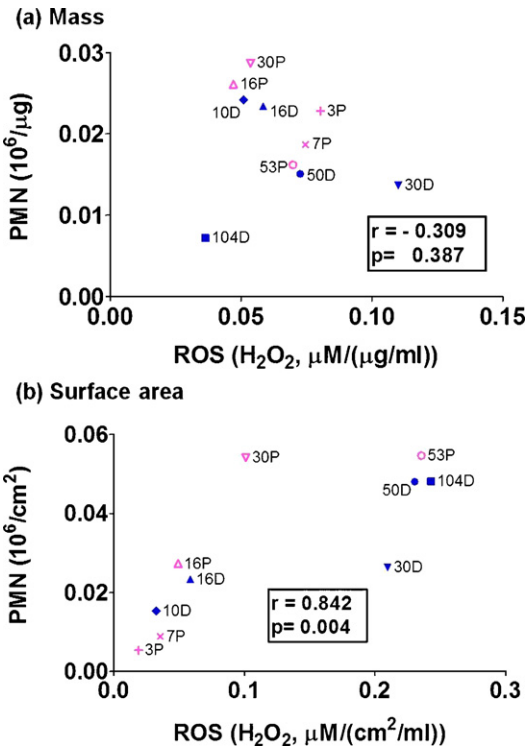

Fig. 10. Spearman correlation between slopes from cell-free ROS data and those from PMN data. When the slopes are based on mass, the correlation is weak with no statistical significance (a); the correlation is strong and significant based on surface area (b). These NPs were prepared using diffusion (marked with "D") or premixed flame method (marked with "P").

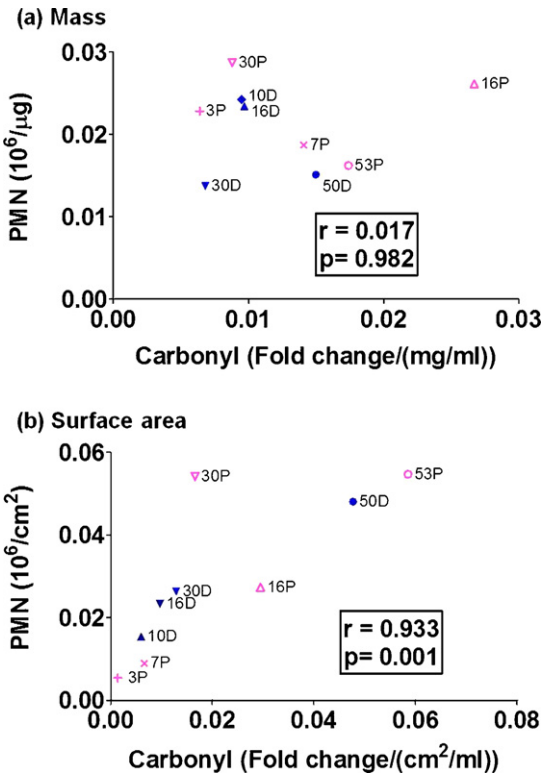

Fig. 12. Spearman correlation between slopes from protein carbonylation data and those from PMN data. When the slopes are based on mass, the correlation is weak with no statistical significance (a); the correlation is strong and significant based on surface area (b). These NPs were prepared using diffusion (marked with "D") or premixed flame method (marked with "P").

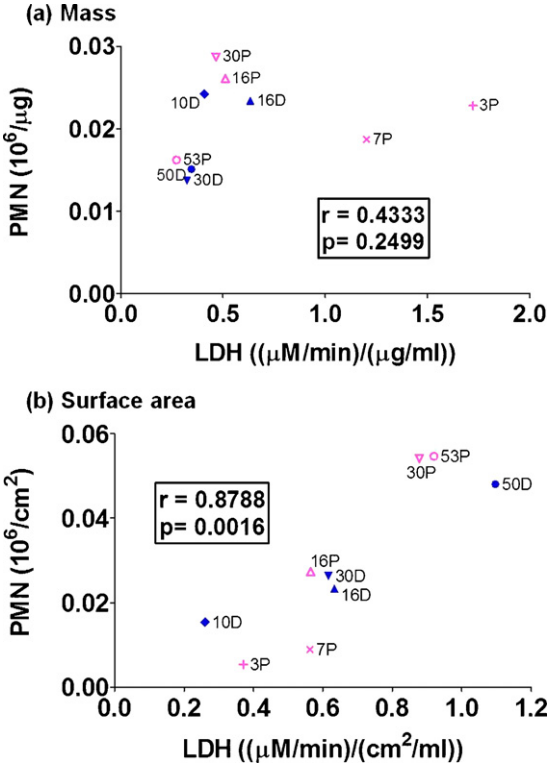

Fig. 11. Spearman correlation between slopes from LDH data and those from PMN data. When the slopes are based on mass, the correlation is weak with no statistical significance (a); the correlation is strong and significant based on surface area (b). These NPs were prepared using diffusion (marked with "D") or premixed flame method (marked with "P").

In characterizing the particles, we found that the hydrodynamic sizes were much larger than particle sizes in dry state (Table 1), indicating that these NPs tend to form agglomerates in the media. Interestingly, the measured sizes of the NPs were about 70% smaller in RPMI medium when 1% FBS was present (Table 1), suggesting that some serum components could partially reverse agglomeration probably by adsorbing onto the surface of the NPs. This finding is in line with the data published by others (Bihari et al., 2008; Allouni et al., 2009; Meissner et al., 2009). In contrast to aggregation of NPs, agglomeration of NPs maintains their surface area (ISO-DIS2011), so the fact that agglomeration of NPs occurred in aqueous solutions justifies the use of surface area as dose metric. It would be desirable, though, to have a measure of biological available surface area, which still needs to be defined.

When correlating *in vitro* results with *in vivo* data, it is critical to find a consistent criterion for comparison. In other words, it is critical to translate the response seen at a certain dose *in vitro* to a corresponding equivalent *in vivo* dose and response.

We addressed this issue by defining the steepest slope of the dose–response curve for toxicity comparison. The main reason for choosing the steepest part of a dose–response curve is that response in this part of the curve is induced by intermediate doses and the response is most sensitive to changes in dose. When doses increase further, the curve becomes less steep as the signal being measured is saturated. This change is consistent with the proposed dose-dependent transitions in mechanisms of toxicity (Slikker et al., 2004). At the lower doses, the response is close to the background response, the response is not very sensitive to a dose change either, yet the response per dose change becomes maximal at the steepest slope.

By obtaining the steepest slope, a whole dose–response dataset is reduced to this single data point. Thus, correlation between two

endpoints could be evaluated based on the steepest slopes for a group of NPs.

Using three *in vitro* and one *in vivo* assay, *in vitro–in vivo* correlations could be correlated based on the steepest slopes. Though not all *in vitro* assays chosen for this study have mechanistic implications, the slope data from the *in vitro* assay show good correlation among themselves (Supplementary information, Tables S-1 and S-2).

When using mass as a dose metric, the correlations were poor with no statistical significance; strong correlations with statistical significance were found when using surface area as the dose metric (Figs. 10–12). This suggests that the *in vitro* assays have predictive values for *in vivo* outcomes, though our work by itself is not a prediction study.

The poor *in vito–in vivo* correlations based on mass do not necessarily indicate a problem with this dose metric since our method should also be applicable to chemicals for which dose metric is not an issue. The poor correlation could be due to the smaller toxicity differences between the NPs when based on mass rather than surface area.

We have explored two methods for calculating the steepest slope. The graphical method is straightforward but there are several limitations when there are only three candidate slopes to choose from – as is the case in our studies – because of only three doses in our *in vivo* animal studies. Firstly, if the steepest slope is not in the middle of the selected dose range, it is conceivable that the slope may be steeper when adding another dose that is outside the current dose range. Secondly, statistical power is limited when using the graphical method. By including data of only two dose groups at a time for calculating slopes and excluding all the other seemingly "irrelevant" groups, the graphical method never takes the full dataset as a whole for statistical analysis. Thirdly, an additional constraint of the method related to the *in vivo* part is the high cost and ethical concerns when conducting animal experiments. Therefore, the mathematical method is preferred where applicable. The criterion to choose between the two methods is to plot the data and examine the shape of the curve to see if it is S-shaped. When in doubt, the mathematical method should be tried first and see if the fitting works.

In the mathematical method, data from all dose groups except the control group and those in an overdosing situation (decreasing response at the high end of the dose–response curve due to decreased viability/increased mortality) are included for statistical analysis, thus leading to increased statistical power. Furthermore, the original data points instead of group means are used for curve fitting (Fig. 4).

While ED_{50} is the traditional means for ranking toxicity for a group of chemicals, the use of the steepest slope is equally appropriate. This is supported by the good correlations between the steepest slopes, ED_{50}, and ED_{10} for some data where ED_{50} and ED_{10} can be calculated (Supplementary information, Tables S-3 and S-4).

However, we did not use ED_{50} for two reasons. First, it is difficult to obtain an ED_{50} for some NPs. For example, if the steepest slope is between the highest dose and the second highest dose, the maximum response cannot be estimated and thus it is impossible to get a reliable ED_{50}. In this case, the mathematical method cannot be used since ED_{50} is needed to use the method. Using the graphical method is the best way available given such a suboptimal situation. Another reason for not using ED_{50} is the linearity of the dose–response curve for the cell-free ROS data from which one cannot get the maximum response. Without the maximum response, one cannot get an ED_{50}.

The NPs chosen in our present study are limited to TiO_2 of different sizes ranging between 3 and 104 nm. But our method is likely to work for other NPs as well even though physico-chemical properties of different types of NPs can be quite diverse. However, when our concept of steepest slope analysis was applied to data reported by Sayes et al. (2007) who evaluated *in vitro* and *in vivo* toxicity of several particles and found that the *in vitro* and *in vivo* results showed poor correlations, our re-analysis using the steepest slope approach showed significant correlations (Rushton et al., 2010).

Furthermore, our preliminary *in vitro–in vivo* correlation study (Rushton et al., 2010) covered 8 different particle types (Rushton et al., 2010) using the same concept as a first proof of principle. Again, significant *in vitro–in vivo* correlations were found which allow developing a hazard scale for toxicity ranking of the different NPs. This is an important step in the risk assessment process.

Still, it is desirable to confirm this concept of steepest slope analysis by conducting similar studies using other NPs of various chemistry and surface modifications. In addition, all endpoints involved in this study were acute endpoints (up to 24 h) and extrapolations to chronic effects are yet to be investigated.

The correlations established between the *in vitro* and *in vivo* assays in this work are non-mechanistic in nature. These empirical correlations are based on statistical analyses and a detailed investigation of the biological relationship between these endpoints is beyond the scope of this work. However the endpoints used in our correlation study (cell-free ROS generation, *in vitro* cellular LDH release, *in vitro* cellular protein carbonylation, and *in vivo* PMN response) are directly or indirectly related to oxidative stress, and therefore are very relevant.

The goal of establishing and verifying *in vitro–in vivo* correlations is an initial step towards predicting *in vivo* toxicity of NPs using validated *in vitro* results. No meaningful predictions can be made for an *in vivo* outcome based on an *in vitro* endpoint that is known to be poorly correlated with the *in vivo* response. Conversely, results of validated *in vitro* assays will be valuable for hazard ranking against well characterized positive and negative reference NPs. Thus, the merit of the steepest slope analysis lies in rapid *in vitro* toxicity screening of nanoparticles for validating *in vitro* assays which are often deemed to be of little relevance due to the use of high doses and other weaknesses.

Conflict of interest

None declared.

Acknowledgments

The authors acknowledge Judy Havalack in the Department of Environmental Medicine, University of Rochester for her skillful assistance in editing this manuscript. This work was supported by AFOSR MURI Grant FA9550-04-1–0430, NSF SGER grant BES-0427262, UR-EPA PM Center Grant RD83241501 and the University of Rochester Toxicology Training Grant T32ES07026, and the NIEHS Center Grant, P30 ESO1247.

Appendix A. Supplementary data

Supplementary data associated with this article can be found, in the online version, at http://dx.doi.org/10.1016/j.tox.2012.03.006.

References

Alamdari, D.H., Kostidou, E., Paletas, K., Sarigianni, M., Konstas, A.G.P., Karapiperidou, A., Koliakos, G., 2005. High sensitivity enzyme-linked immunosorbent assay (ELISA) method for measuring protein carbonyl in samples with low amount of proteins. Free Radical Biology & Medicine 39, 1362–1367.

Allouni, Z.E., Cimpan, M.R., Hol, P.J., Skodvin, T., Gjerdet, N.R., 2009. Agglomeration and sedimentation of TiO_2 nanoparticles in cell culture medium. Colloids and Surfaces B: Biointerfaces 68, 83–87.

Belyanskaya, L., Manser, P., Spohn, P., Bruinink, A., Wick, P., 2007. The reliability and limits of the MTT reduction assay for carbon nanotubes–cell interaction. Carbon 45, 2643–2648.

Bihari, P., Vippola, M., Schultes, S., Praetner, M., Khandoga, A.G., Reichel, C.A., Coester, C., Tuomi, T., Rehberg, M., Krombach, F., 2008. Optimized dispersion of nanoparticles for biological *in vitro* and *in vivo* studies. Particle and Fibre Toxicology 5, 14–27.

Brown, D.M., Wilson, M.R., MacNee, W., Stone, V., Donaldson, K., 2001. Size-dependent proinflammatory effects of ultrafine polystyrene particles: a role for surface area and oxidative stress in the enhanced activity of ultrafines. Toxicology and Applied Pharmacology 175, 191–199.

Brunauer, S., Emmett, P.H., Teller, E., 1938. Adsorption of gases in multimolecular layers. Journal of the American Chemical Society 60, 309–319.

Buss, I.H., Chan, T.P., Sluis, K.B., Domigan, N.M., Winterbourn, C.C., 1997. protein carbonyl measurement by a sensitive ELISA method. Free Radical Biology & Medicine 23, 361–366.

Casey, A., Herzog, E., Davoren, M., Lyng, F.M., Byrne, H.J., Chambers, G., 2007. Spectroscopic analysis confirms the interactions between single walled carbon nanotubes and various dyes commonly used to assess cytotoxicity. Carbon 45, 1425–1432.

Federici, G., Shaw, B.J., Handy, R.D., 2007. Toxicity of titanium dioxide nanoparticles to rainbow trout (*Oncorhynchus mykiss*): gill injury, oxidative stress, and other physiological effects. Aquatic Toxicology 84, 415–430.

Guo, L., Von Dem Bussche, A., Buechner, M., Yan, A., Kane, A.B., Hurt, R.H., 2008. Adsorption of essential micronutrients by carbon nanotubes and the implications for nanotoxicity testing. Small 4, 721–727.

Han, X., Gelein, R., Corson, N., Wade-Mercer, P., Jiang, J., Biswas, P., Finkelstein, J.N., Elder, A., Oerdorster, G., 2011. Validation of an LDH assay for assessing nanoparticle toxicity. Toxicology 287, 99–104.

Hussain, S.M., Hess, K.L., Gearhart, J.M., Geiss, K.T., Schlager, J.J., 2005. *In vitro* toxicity of nanoparticles in BRL 3A rat liver cells. Toxicology In Vitro 19, 975–983.

Jiang, J., Chen, D., Biswas, P., 2007. Synthesis of nanoparticles in a flame aerosol reactor with independent and strict control of their size, crystal phase and morphology. Nanotechnology 18, 285603.

Jiang, J., Oberdörster, G., Elder, A., Gelein, R., Mercer, P., Biswas, P., 2008. Does nanoparticle activity depend upon size and crystal phase? Nanotoxicology 2, 33–42.

Koslowski, R., Barth, K., Augstein, A., Tschernig, T., Bargsten, G., Aufderheide, M., Kasper, M., 2004. A new rat type I-like alveolar epithelial cell line R3/1: bleomycin effects on caveolin expression. Histochemistry and Cell Biology 121, 509–519.

Limbach, L.K., Wick, P., Manser, P., Grass, R.N., Bruinink, A., et al., 2007. Exposure of engineered nanoparticles to human lung epithelial cells: influence of chemical composition and catalytic activity on oxidative stress. Environmental Science and Technology. 41, 4158–4163.

Long, T.C., Saleh, N., Tilton, R.D., Lowry, G.V., Veronesi, B., 2006. Titanium dioxide (p25) produces reactive oxygen species in immortalized brain microglia (bv2): implications for nanoparticle neurotoxicity. Environmental Science and Technology 40, 4346–4352.

Meissner, T., Potthoff, A., Richter, V., 2009. Suspension characterization as important key for toxicological Investigations. Nanosafe 2008: International Conference on Safe Production and Use of Nanomaterials. Journal of Physics: Conference Series 170, 012012.

Monteiller, C., Tran, L., MacNee, W., Faux, S., Jones, A., Miller, B., Donaldson, K., 2007. The pro-inflammatory effects of low-toxicity low-solubility particles, nanoparticles and fine particles, on epithelial cells *in vitro*: the role of surface area. Occupational and Environmental Medicine 64, 609–615.

Nel, A.E., Xia, T., Mädler, L., Li, N., 2006. Toxic potential of materials at the nanolevel. Science 311, 622–627.

Oberdörster, G., Maynard, A., Donaldson, K., Castranova, V., Fitzpatrick, J., Ausman, K., Carter, J., Karn, B., Kreyling, W., Lai, D., et al., 2005a. Principles for characterizing the potential human health effects from exposure to nanomaterials: Elements of a screening strategy. Particle and Fibre Toxicology 2, 8–42.

Oberdörster, G., Oberdörster, E., Oberdörster, J., 2005b. Nanotoxicology: an emerging discipline involving from studies of ultrafine particles. Environmental Health Perspectives. 113, 823–839.

Oberdörster, G., Oberdörster, E., Oberdörster, J., 2007. Concepts of nanoparticle dose metric and response metric. Environmental Health Perspectives 115, A290.

Park, M.V., Lankveld, D.P., van Loveren, H., de Jong, W.H., 2009. The status of *in vitro* toxicity studies in the risk assessment of nanomaterials. Nanomedicine 4, 669–685.

Rushton, E.K., Jiang, J., Leonard, S., Eberly, S., Castranova, V., Biswas, P., Elder, A., Han, X., Gelein, R., Finkelstein, J., Oberdörster, G., 2010. Concept of assessing nanoparticle hazards considering nanoparticle dosemetric and chemical/biological response-metrics. Journal of Toxicology and Environmental Health Part A 73, 445–461.

Sayes, C.M., Wahi, R., Kurian, P.A., Liu, Y., West, J.L., Ausman, K.D., et al., 2006. Correlating nanoscale titania structure with toxicity: a cytotoxicity and inflammatory response study with human dermal fibroblasts and human lung epithelial cells. Toxicological Sciences 92, 174–185.

Sayes, C.M., Reed, K.L., Warheit, D.B., 2007. Assessing toxicity of fine and nanoparticles: comparing in vitro measurements to in vivo pulmonary toxicity profiles. Toxicological Sciences 97, 163–180.

Seagrave, J., McDonald, J.D., Mauderly, J.L., 2005. *In vitro* versus *in vivo* exposure to combustion emissions. Experimental and Toxicologic Pathology 57, 233–238.

Slikker Jr., W., Andersen, M.E, Bogdanffy, M.S., Bus, J.S., Cohen, S.D., Conolly, R.B., David, R.M., Doerrer, N.G., Dorman, D.C., Gaylor, D.W., Hattis, D., Rogers, J.M., Setzer, R.W., Swenberg, J.A., Wallace, K., 2004. Dose-dependent transitions in mechanisms of toxicity. Toxicology and Applied Pharmacology 201, 203–225.

Stahl, P.D., Fishman, W.H., 1984. b-D-Glucuronidase. In: Bergmeyer, J., Grassl, M. (Eds.), Methods in enzymatic analysis, vol. 5. Verlag Chemie, Weinheim, p. 246.

Stern, S.T., McNeil, S.E., 2008. Nanotechnology safety concerns revisited. Toxicological Sciences 101, 4–21.

Stoeger, T., Schmid, O., Takendaka, S., Schulz, H., 2007. Inflammatory response to tio2 and carbonaceous particles scales best with bet surface area. Environmental Health Perspectives 115, A290–A291.

Teeguarden, J.G., Hinderliter, P.M., Orr, G., Thrall, B.D., Pounds, J.G., 2007. Particokinetics *in vitro*: dosimetry considerations for *in vitro* nanoparticle toxicity assessments. Toxicological Sciences 95, 300–312.

Wittmaack, K., 2007. In search of the most relevant parameter for quantifying lung inflammatory response to nanoparticle exposure: particle number surface area, or what? Environmental Health Perspectives 115, 187–194.

Wörle-Knirsch, J.M., Pulskamp, K., krug, H.F., 2006. Oops they did it again! carbon nanotubes hoax scientists in viability assays. Nano Letters 6, 1261–1268.

Xiao, G.G., Wang, M., Li, N., Loo, J.A., Nel, A.E., 2003. Use of proteomics to demonstrate a hierarchical oxidative stress response to diesel exhaust particle chemicals in a macrophage cell line. Journal of Biological Chemistry 278, 50781–50790.